Dynamical Event during Slow Crack Propagation

Knut Jørgen Måløy[1] and Jean Schmittbuhl[2]

[1]*Fysisk Institutt, Universitetet i Oslo, P.O. Boks 1048 Blindern, N-0316 Oslo 3, Norway*

[2]*Laboratoire de Géologie, UMR 8538 École Normale Supérieure, 24 rue Lhomond, 75231 Paris Cedex 05, France*

(Received 29 January 2001; published 17 August 2001)

We address the role of material heterogeneities on the propagation of a slow rupture at laboratory scale. With a high speed camera, we follow an in-plane crack front during its propagation through a transparent heterogeneous Plexiglas block. We obtain two major results. First, the slip along the interface is strongly correlated over scales much larger than the asperity sizes. Second, the dynamics is scale dependent. Locally, mechanical instabilities are triggered during asperity depinning and propagate along the front. The intermittent behavior at the asperity scale is in contrast with the large scale smooth creeping evolution of the average crack position. The dynamics is described on the basis of a Family-Vicsek scaling.

DOI: 10.1103/PhysRevLett.87.105502 PACS numbers: 62.20.Mk, 46.50.+a, 61.43.–j, 81.40.Np

Most studies on fractures have focused on homogeneous materials. The role of heterogeneities has been addressed more recently. For instance, heterogeneities lead to self-affine long range correlations of fracture roughness [1,2]. However, the physical influence of heterogeneities on the crack process is still not fully understood. Static elasticity leads to long range interactions along the crack front [3,4] but additional elastic waves, especially recently observed crack front waves [5,6], create dynamical stress overshoots which play an important role. In most modeling of fracture dynamics in heterogeneous materials, especially at low speed, the latter are ignored since a quasistatic assumption is used. Actually very few experimental data that describe the crack front propagation through heterogeneous materials exist. This work presents *the very first experiment* where the detailed dynamics of a fracture front line in a heterogeneous material is investigated. At large scales, seismic inversions of slip history during an earthquake [7] provide hints of the features of the rupture front but with a low resolution, especially compared to the heterogeneity sizes (i.e., asperities). At laboratory scales, a 3D description of a crack front at rest in a heterogeneous aluminum alloy was obtained by Daguier *et al.* [2].

Interesting similarities exist between the propagation of crack fronts through a heterogeneous medium and the problem of propagation of dislocation lines through a field of solute atoms. At low temperatures, the dislocation lines become rough due to pinning by immobile solute atoms [8–10] adjusting its shape to the local stress.

We describe here an experiment where two Plexiglas plates are annealed together to create a single block with a weak interface [11]. Propagation of the crack front along the weak interface is directly observable because of the transparency of the material. The plates are as follows: 32 cm $\times$ 14 cm $\times$ 1 cm and 34 cm $\times$ 12 cm $\times$ 0.4 cm, and annealed together at 205 °C under several bars of normal pressure. Before annealing, both plates are sandblasted on one side with 50 μm steel particles. Sandblasting introduces a random topography which induces local toughness fluctuations during the annealing procedure. The upper Plexiglas plate is clamped to a stiff aluminum frame. A normal displacement is applied by a press to the lower plate which results in a stable crack propagation in mode I at constant low speed (68 μm/s) [12]. The fracture front is observed with a microscope linked to a high speed Kodak Motion Korder Analyzer camera which records during 8.7 s at 500 images per second with a 512 $\times$ 240 pixel resolution (1 pixel covers an area of 10 μm $\times$ 10 μm). In Fig. 1 is shown a sample image obtained with this setup where the front is observed from above. The uncracked part is seen as white (i.e., transparent), while the gray region represents the open fracture (i.e., nontransparent since the sandblasting procedure unpolishes the surfaces). The front is defined as the contrast boundary. The x and y coordinates are defined in Fig. 1. The front line position is given by $y = a(x, t)$. In Fig. 1, samples of fronts separated with a constant time interval $dt = 200$ ms are superimposed on the picture. Local fluctuations of the front movement can be seen from the variations in the distance between the front lines. We define a front normal $\vec{n}$ to be normal to the front line and

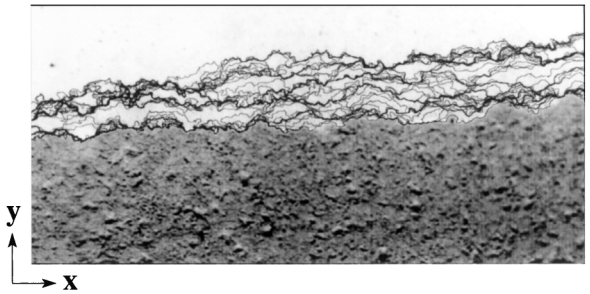

FIG. 1. Sample of crack fronts. The background is an inverted raw image covering an area of 5.12 mm $\times$ 2.4 mm where the intact material appears white. In contrast, the cracked zone is dark. Crack propagates in this case from bottom to top (x direction) because of a tensile mode I load. The 43 solid lines that correspond to the fracture front positions for later times are superimposed on the picture. The time delay between each front is 200 ms. Totally 4367 pictures were taken with a time interval of 2 ms between each picture in this experiment.

with a positive direction into the uncracked region. Let V be the local front velocity in the direction of the front normal. The velocities V at all front positions were calculated by measuring the distance δl, along the normal, to the intersection with the front that is 20 ms later. The distributions of the velocity components $V_y = V\vec{n} \cdot \vec{e}_y$ and $V_x = V\vec{n} \cdot \vec{e}_x$, respectively, parallel and perpendicular to the global fracture propagation direction, are shown in Fig. 2. Here $\vec{e}_y$ and $\vec{e}_x$ are the unit vectors in the y and x directions, respectively.

Figure 3 shows the position fluctuations of the crack front: $\delta a(x,t) = a(x,t) - \langle a(x,t)\rangle_x$ in gray levels. Dark grays correspond to pinned regions of the front that evolve slower than the average crack front ($\delta a \ll 0$). On the contrary, light regions are in advance ($\delta a \gg 0$). In Fig. 3b are plotted the position fluctuations in the space-space diagram which illustrate the richness of the crack propagation dynamics. Black areas are asperities where the front is stopped. Arrest periods are localized in space but of any size and followed by an overshoot propagation that appears in white. Figure 3a is a space-time diagram of the same front position fluctuations. Two main aspects of the figure have to be emphasized. First there are numerous sharp transitions that appear close to horizontal and very localized in time. They are triggered after pinning periods (black regions) and clearly correspond to fast propagation of dynamical events because of local mechanical instabilities along the front. The second main feature of the figure is the column aspect which illustrates the dynamics of the crack propagation. Crack front position evolves only because of the instabilities. Apart from them, there is almost no evolution of the crack shape.

The dynamic scaling of the fracture front has been checked by calculating the power spectrum $P(k,t)$ of the position difference $\Delta a(x,t) = a(x,t) - a(x,t=0)$, where k is the wave number and t is the time ($t = 0$ corresponds to the first image). The Family-Vicsek scaling [13] of the power spectrum $P(k,t)$ can be written as

$$P(k,t) = t^{(1+2\zeta)/\kappa} G(kt^{1/\kappa}), \qquad (1)$$

where $G(x)$ is constant for $x \ll 1$ and $G(x) \propto x^{-1-2\zeta}$ for $x \gg 1$. The dynamic exponent κ gives the scaling with time of the correlation length that separates both domains $\xi_x \propto t^{1/\kappa}$. Many self-affine growth models [14], fracture models [4], and experiments [14–16] have been found to exhibit Family-Vicsek scaling. In Fig. 4a, the power spectrum of the relative position $\Delta a(x,t)$ is shown at different times from 0.03 to 7.11 s. At small times, no spatial correlation exists and the spectrum appears flat. For larger times, however, the correlations become apparent, and a crossover to a power law behavior is observed for large k. For large times data are consistent with a power law: $P(k) \propto k^{-1-2\zeta}$ with $\zeta = 0.6$. The latter value of the roughness exponent has been extensively checked for fronts at rest over a larger range of scales (5 μm to 50 mm) [11]. This shows that the front roughness is strongly correlated over a large range of scales significantly larger than the asperity sizes controlled by the sandblasting particles (50 μm). In Fig. 4b, the scaling function $P(k,t)t^{(-1-2\zeta)/\kappa}$ is plotted as a function of $kt^{1/\kappa}$. This data collapse provides an estimate of the dynamic exponent $\kappa = 1.2$. We emphasize that the exponent might be different from the dynamic exponent obtained from an initially flat front. However, the subtraction technique presented here is the only one experimentally accessible.

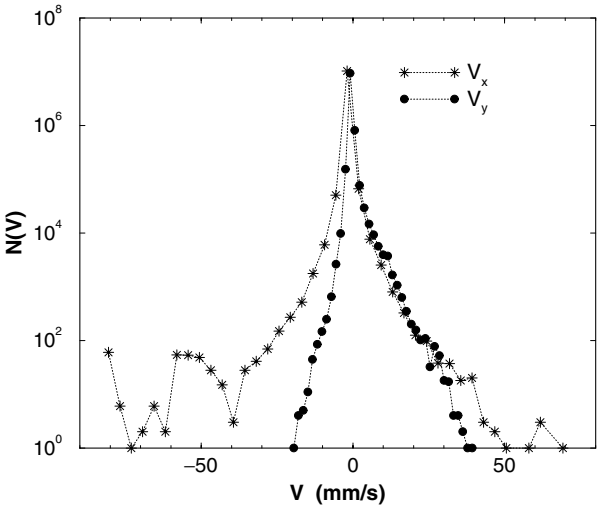

FIG. 2. Distributions of the velocity components V_x and V_y in a linear-log diagram. Distribution tails are shown to decrease slower than exponential. Velocities are calculated on the basis of fronts separated with a time interval of $\delta t = 20$ ms. The largest measured local speeds are 3 orders of magnitude larger than the average front speed $V_f = 68$ μm/s. It is important to note that the speeds V_x and V_y are average speeds within the time $\delta t = 20$ ms. Much higher speed fluctuations may be present. Because of front overhangs the local speed fluctuations V_y may also be negative as seen in the distribution.

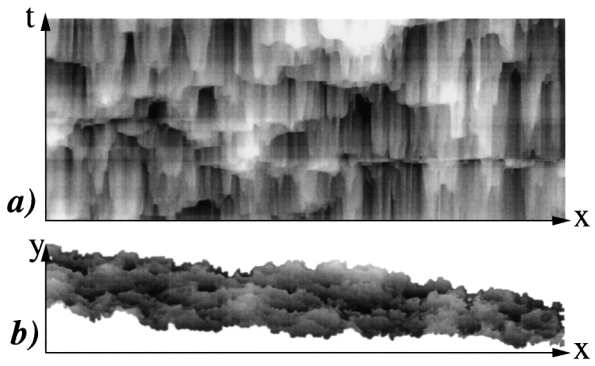

FIG. 3. (a) The figure shows the space-time (x,t) diagram (5.12 mm × 8.7 sec) of the position fluctuations with respect to the average position of the front $\delta a(x,t) = a(x,t) - \langle a(x,t)\rangle_x$ using gray levels. Light gray corresponds to positive values of δa, while dark gray corresponds to negative values of δa. (b) A similar gray level representation as in (a) but the space-space coordinates $(x, a(x,t))$. The image covers an area of 5.12 mm × 1.08 mm.

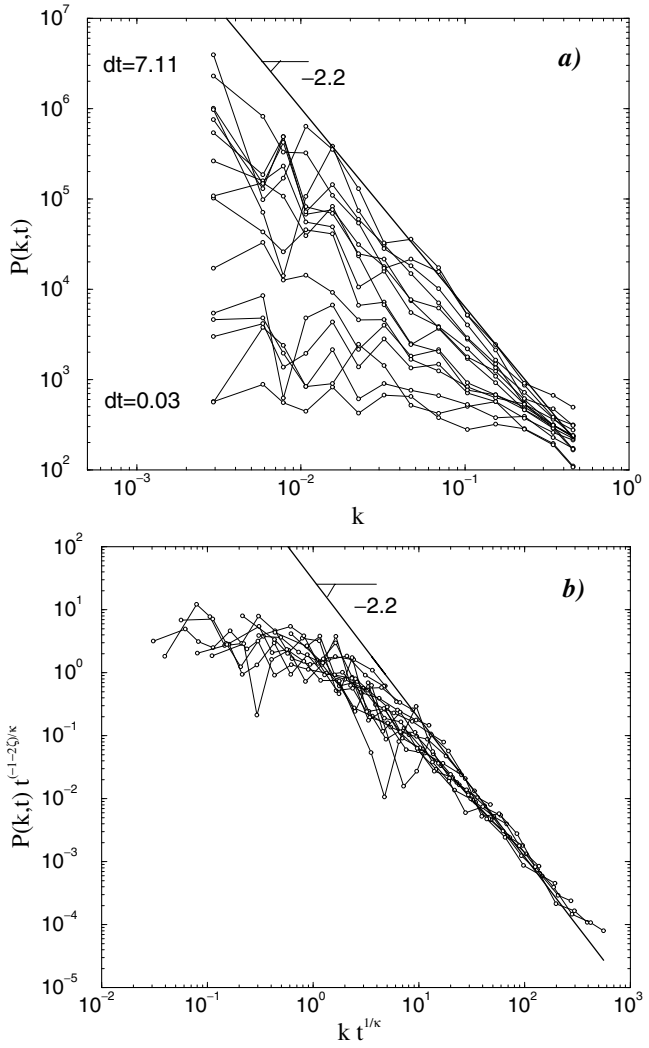

FIG. 4. (a) The power spectrum $P(k,t)$ of the front position fluctuations $\Delta a = a(x,t) - a(x,t=0)$ plotted as a function of the wave number k. (b) Family-Vicsek scaling: The dependence of the scaling function $P(k,t)t^{-(1+2\zeta)/\kappa}$ with $kt^{1/\kappa}$. This data collapse shows the growth of the correlation length (or crossover length) with time, $\zeta_x \propto t^{1/\kappa}$, and gives an estimate of the dynamic exponent $\kappa = 1.2$.

The roughness exponents obtained in our experiment are not consistent with most present relevant theoretical models or simulations [4,5,10,17]. The solution of the quasistatic elastic in-plane crack problem for an initially flat front propagating in a heterogeneous plane gives the roughness exponent $\zeta = 0.35$ and the dynamic exponent $z = 0.75$ [4] different from the experimental results ($\zeta = 0.60$ and $\kappa = 1.2$). However, the experimental results are closer to a recent theoretical model proposed by Ramanathan and Fisher [5] in which they solve the elastic problem of a planar tensile crack in a heterogeneous medium with a full elastodynamic description. In the ideal case where the toughness is not dependent on the velocity, they predict a roughness exponent $\zeta = 0.5$. This model contains elastic waves, and in particular crack front waves [5,6] which will create stress overshoot along the fracture front. Stress overshoot [5,6,18] may be responsible for instabilities and might explain why we observe in our experiments a very significant amplification of the localized front propagation velocities along the fracture line even for a very slow average propagation. Another approach (self-organized depinning) has been proposed by Sneppen [19] where the front line is moved in a quenched disorder. The pinning is nonlocal because of propagation along the front to equilibrate the local slope. Surprisingly, the latter model provides a very close estimate of the roughness exponent $\zeta = 0.63$ but an underestimate of the dynamical exponent $z = 0.7$.

Strong analogies exist between crack propagation and friction [20]. For both phenomena, the evolution of the mechanical potential energy balances that of the rupture propagation resistance (surface energy) and that of the kinetic energy. We observed (see Fig. 3b) that instabilities at the depinning transition transform a smooth slow movement of the rupture at large scale to local stick-slip motions of the crack front. Sticks correspond to periods of asperity pinning (black areas) and slip to the asperity depinning (white areas) including a sidewise propagation along the front. The latter are dynamical effects that control most of the crack propagation. An open question is to define the range of scales over which the dynamical effects influence the crack advance and more specifically if there exist time and space cutoffs above which a quasistatic approach might be successful. As shown from this study, crack front velocity fluctuates significantly both in space and time: over 2 orders of magnitude in space and 3 orders of magnitude in time (see Fig. 3). Accordingly, the definition of crack speed average is scale dependent and therefore questionable.

Stick-slip motion is very well documented for solid friction experiments [21]. Dynamical effects during friction instability (slip weakening, velocity weakening, or rate and state friction laws) exist and are responsible for the slip history. For crack propagation, dynamical effects on the toughness (e.g., toughness sensitivity on crack velocity) are also shown to exist [22]. Moreover, elastic wave propagation (especially crack front waves) that involves the lowest time scales might also influence the propagation for both phenomena. Because of the speed measurement limitations (in the range from 6×10^{-6} to 2.5×10^{-1} m/s), all ranges of dynamical effects are not accessible with our setup. For instance, distinction between processes involving fast evolution of the local rupture resistance and wave propagation is difficult. No process zone at the crack tip was observed in the experiment above the micrometer scale (light wavelength). However, process zones are shown to influence significantly the crack geometry [22,23].

Upscaling of the experimental results to fault mechanics might provide useful informations on asperity interactions along the fault plane and new insights for the actual behavior of creeping faults. Recent observations show strong space correlations of the seismic activity along creeping

faults [24]. Our results are consistent with the latter observations. We show that the slip is correlated along the interface on a scale much larger than the asperity size. This is of great importance for the interpretation of rupture heterogeneities in terms of large scale geological asperities from long wavelength inversion of INSAR (interferometric synthetic aperture radar) or GPS (global positioning system) or strong motion data [7,25]. We also show that the dynamics at the asperity scale is very different from that at large scale. The creep behavior observed at large scale is negligible at local scale. Dynamical events are initiated during depinning and propagate along the rupture front even if the loading at large scale is very slow. Such local mechanical instabilities or microquake are intermittent but strongly correlated both in time and space and are responsible for most of the large scale deformation.

We thank R. Madariaga, J. Rice, A. Hansen, S. Roux, J. P. Vilotte, E. Flekkøy, J. Lothe, and J. J. Ramasco for fruitful discussions. This work was supported by the CNRS programs "ECODEV" and "Intérieur de la Terre," the CNRS/NFR PICS program, and the NFR Grant No. 135416/410.

[1] B. B. Mandelbrot, D. E. Passoja, and A. J. Paullay, Nature (London) **308**, 721 (1984); S. R. Brown and C. H. Scholz, J. Geophys. Res. **90**, 12 575 (1985); J. Schmittbuhl, S. Gentier, and S. Roux, Geophys. Res. Lett. **20**, 639 (1993); B. L. Cox and J. S. Y. Wang, Fractals **1**, 87 (1993); K. J. Måløy, A. Hansen, E. L. Hinrichsen, and S. Roux, Phys. Rev. Lett. **68**, 213 (1992); J. Schmittbuhl, F. Schmitt, and C. H. Scholz, J. Geophys. Res. **100**, 5953 (1995).

[2] P. Daquier, E. Bouchaud, and G. Lapasset, Europhys. Lett. **31**, 367 (1995).

[3] H. Gao and J. R. Rice, ASME J. Appl. Mech. **56**, 828 (1989).

[4] J. Schmittbuhl, S. Roux, J. P. Vilotte, and K. J. Måløy, Phys. Rev. Lett. **74**, 1787 (1995).

[5] S. Ramanathan and D. Fisher, Phys. Rev. B **58**, 6026 (1998); S. Ramanathan and D. Fisher, Phys. Rev. Lett. **79**, 877 (1997).

[6] J. W. Morrisey and J. R. Rice, J. Mech. Phys. Solids **48**, 1229 (2000); J. Mech. Phys. Solids **46**, 467 (1998); E. Sharon, G. Cohen, and J. Fineberg, Nature (London) **410**, 68 (2001).

[7] K. B. Olsen, R. Madariaga, and R. J. Archuleta, Science **278**, 834 (1997); B. Hernandez, F. Cotton, and M. Campillo, J. Geophys. Res. **104**, 13 083–13 099 (1999); M. Bouchon *et al.,* Geophys. Res. Lett. **27**, 3013 (2000).

[8] N. F. Mott and F. R. N. Nabarro, Proc. R. Soc. London **52**, 86 (1940).

[9] J. P. Hirth and J. Lothe, *Theory of Dislocations* (Wiley-Interscience, New York, 1982).

[10] S. Roux and A. Hansen, J. Phys. I **4**, 515 (1994).

[11] J. Schmittbuhl and K. J. Måløy, Phys. Rev. Lett. **78**, 3888 (1997); A. Delaplace, J. Schmittbuhl, and K. J. Måløy, Phys. Rev. E **60**, 1337 (1999); J. Schmittbuhl, A. Delaplace, and K. J. Måløy, *In Physical Aspects of Fracture,* edited by E. Bouchaud (Kluwer Academic Publishers, Dordrecht, 2001).

[12] The critical stress intensity factor for a crack propagation along the interface has been measured as 90 kPa $m^{1/2}$ which is 500 times smaller than the critical stress intensity factor for a propagation in the bulk.

[13] F. Family and T. Vicsek, J. Phys. A **18**, L75 (1985).

[14] A. L. Barabasi and H. E. Stanley, *Fractal Concepts in Surface Growth* (Cambridge University Press, New York, 1995).

[15] V. K. Horvath, F. Family, and T. Vicsek, J. Phys. A **24**, L25 (1991).

[16] C. Thompson, C. Palasantzas, Y. P. Feng, S. K. Sinha, and J. Krim, Phys. Rev. B **49**, 4902 (1994).

[17] J. P. Bouchaud, E. Bouchaud, G. Lapasset, and J. Planes, Phys. Rev. Lett. **71**, 2240 (1993).

[18] L. C. Krysac and J. D. Maynard, Phys. Rev. Lett. **81**, 4428 (1998).

[19] K. Sneppen, Phys. Rev. Lett. **69**, 3539 (1992).

[20] B. K. Atkinson, *Fracture Mechanics of Rocks* (Academic Press, London, 1991).

[21] N. J. Persson, *Sliding Friction: Physical Principles and Applications* (Springer-Verlag, Berlin, 1998); C. H. Scholz, *The Mechanics of Earthquakes and Faulting* (Cambridge University Press, New York, 1990).

[22] B. Lawn, *Fracture of Brittle Solids* (Cambridge University Press, Cambridge, U.K., 1993), 2nd ed.; J. Fineberg and M. Marder, Phys. Rep. **313**, 1 (1999).

[23] S. Zapperi, H. J. Herrmann, and S. Roux, Eur. Phys. J. B **17**, 131 (2000).

[24] A. M. Rubin, D. Gillard, and J. L. Got, Nature (London) **400**, 635 (1999).

[25] H. Perfettini, J. Schmittbuhl, and J. P. Vilotte, Geophys. Res. Lett. **28**, 2133 (2001).